JCTC Journal of Chemical Theory and Computation

pubs.acs.org/JCTC Article

Screened Range-Separated Hybrid Functional with Polarizable Continuum Model Overcomes Challenges in Describing Triplet Excitations in the Condensed Phase Using TDDFT

Khadiza Begam, Srijana Bhandari, Buddhadev Maiti, and Barry D. Dunietz*

Cite This: https://dx.doi.org/10.1021/acs.jctc.0c00086 Read Online

ACCESS | Metrics & More | Article Recommendations | Supporting Information

ABSTRACT: Long range-corrected (LRC) or range-separated hybrid (RSH) functionals where the long-range (LR) limit of electronic interactions is set to the exact exchange have been shown to correct the tendency of traditional density functional theory (DFT) to underestimate the frontier orbital gap. Consequently, the use of such functionals in calculating electronic excited states using linear response based time-dependent DFT (TDDFT) has been successful in correcting the tendency for underestimating the energies of charge transfer states by DFT-based calculations. More recently formulations of functionals that attenuate the LR limit to address condensed-phase effects to polarize the electronic density have been reported. In particular screened RSH (SRSH) combined with polarizable continuum model (PCM) was benchmarked successfully in reproducing the fundamental gap and charge transfer state energies of molecular systems in the condensed phase. Here we use SRSH-PCM to address triplet excited states, and show its success in obtaining correspondence of the low-lying triplet states to the singlet−triplet gap in a similar way that the fundamental orbital gap corresponds to electron removal and addition energies. Importantly, the accuracy of the SRSH-PCM in calculating triplet excitations stands on the polarization consistent framework in addressing the scalar dielectric constant and *without* affecting the optimal tuning by triplet energies. The prospect of even further improving the SRSH-PCM accuracy in calculating triplet states can be achieved by optimal tuning on the basis of the spin multiplicity gap.

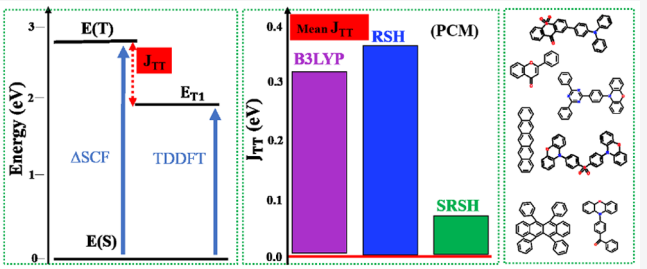

INTRODUCTION

Organic semiconducting materials are widely considered for optoelectronic applications, as of organic light emitting diodes (OLEDs), due to their tunability and relative low cost.[1−3] Emerging applications based on triplet electronic excitations in organic materials include solar energy harvesting using singlet fission, high-resolution displays, white color lighting diode, and bioimaging.[4−7] Indeed, recent OLEDs based on thermally activated delayed fluorescence (TADF) have transformed consumer electronics over the past decade.[8−10] These recent advances underscore the need for computational tools for designing the materials, where the excitation energies of the low-lying singlet and triplet electronic states are controlled to enhance the device efficiency. Primarily, computational studies that aim to contribute to relevant design efforts must address reliably the effect of the condensed-phase environment on the material optical properties.

Linear response formulation of time-dependent density functional theory (TDDFT)[11−15] is the most employed level of first-principles electronic structure theory for calculating electronic excited states. However, traditional DFT-based calculations are associated with several artifacts that limit the reliable applicability of the approach.[16−19] Crucially these limitations are in the treatment of charge transfer (CT) and Rydberg and triplet excitations that are all usually addressed with reservation when calculated by DFT.[20−22]

Nevertheless, over the past decade functionals based on enforcing the long-range limit of exact exchange have been developed and have shown great success in addressing the shortcoming of DFT in describing CT states.[23−27] Of importance are Coulomb attenuated functionals that distinguish between long range (LR) and short range (SR) in the assigned weight of the exact exchange. In particular, of interest are optimally tuned (OT) range-separated hybrid (RSH) functionals[26,28,29] with a range switching parameter that establish the Koopmans theorem[30,31] for DFT, where the highest occupied molecular orbital (HOMO) energy corresponds to the ionization potential ([IP], which is a required property of the exact, while unknown, functional) and the lowest unoccupied molecular orbital (LUMO) energy corresponds to the electron affinity (EA). Clearly functionals

Received: January 24, 2020

https://dx.doi.org/10.1021/acs.jctc.0c00086
J. Chem. Theory Comput. XXXX, XXX, XXX−XXX

that are associated with such physically significant frontier orbitals contribute to the success of TDDFT in describing properly CT states.

More recently, RSH functionals were adapted to address the condensed-phase environment. Toward this goal, RSH formulation was developed for molecular systems in the solid phase using the periodic framework of DFT.[32−34] Similar success has been reported by affecting the LR limit by screening the exact exchange.[34−38] Screened RSH (SRSH) in combination with polarizable continuum model (PCM), SRSH-PCM, is especially promising as it was found to reproduce well the fundamental orbital gap of molecular systems in the condensed phase[38] and in addressing CT states in solvated donor−acceptor complexes.[39] The success of SRSH-PCM stems from its polarization consistent aspect, where the electrostatic environment is represented by the scalar dielectric constant (ϵ). In SRSH-PCM the same screened interactions are imposed in the functional parameters and in the PCM treatment. Namely, the same ϵ is affected both in setting the functional parameters that determine the weight of LR exact exchange and in the self-consistent reaction field iterations of the PCM.[38,40]

In this report we turn to use SRSH-PCM for addressing triplet excitations. However, TDDFT calculations can be affected by the infamous triplet instability affecting DFT, especially in cases with dominant exact exchange contributions.[41−45] In such cases the triplet eigenvalues obtained by the linear response TDDFT calculations tend to be underestimated in comparison to the spin multiplicity energy gap (if not becoming imaginary). Below we demonstrate the success of the SRSH-PCM-based TDDFT framework to eliminate the deviation of the triplet excitations from the gap energies and especially when affected by the polarizable environment that is expected to greatly affect the optoelectronic properties. We consider a benchmark set of molecules that comprise some of the *usual suspects* that are widely employed in optoelectronic applications and for which there are measured excitation energies to compare against. *Indeed, in this report, we first demonstrate the success of the SRSH-PCM approach to eliminate the numerical instability affecting triplet excitation energies in TDDFT calculations and then confirm the predictive quality of the calculated energies by comparing against measured energies.*

COMPUTATIONAL APPROACH

The success of the OT-RSH framework in describing CT states appears to also improve the treatment of triplet excitations.[7,34,36,43,46−48] Indeed attenuated Coulomb-based functionals, where the exact exchange weight varies between the LR and SR, have been shown to address well the singlet−triplet gap.[7,43] More recently Lin and Van Voorhis have shown that triplet excitations can be further improved by tuning the functional parameters in the spirit of optimally tuning the distance parameter in RSH for the orbital energies, where a triplet-tuning (TT) measure is defined.[49] The TT error measure based on triplet energies is as follows:

$$J_{\mathrm{TT}} = \|\Delta E_{\mathrm{st}}(\mathrm{SCF}) - E_{\mathrm{T1}}\| \tag{1}$$

where $\Delta E_{\mathrm{st}}(\mathrm{SCF})$ is the singlet−triplet self-consistent field (SCF) energies gap and E_{T1} is the lowest triplet excited state calculated using TDDFT (on the basis of the same functional).[49]

In this report we turn to address triplet states in the condensed-phase system using the polarization consistent SRSH-PCM framework, which was recently introduced. We demonstrate the success of the SRSH-PCM framework to obtain consistency between the singlet−triplet energy gap and the triplet excitation energy. In this study, the J_{TT} measure defined in eq 1 is used *primarily* as a quality measure for the calculated triplet energies similar to the J_{OT}, reflecting the quality of calculated CT states. We contrast the J_{TT} error measure in calculating triplet excited states in the condensed phase by SRSH-PCM to those obtained by alternative functionals and by HF with PCM. We note that functional tuning based on triplet energies may be invoked for tightening the accuracy.

SRSH framework is based on partitioning the electronic interactions into LR and SR using an error function (erf):

$$\frac{1}{r} = \frac{\alpha + \beta\ \mathrm{erf}(\omega r)}{r} + \frac{1 - (\alpha + \beta\ \mathrm{erf}(\omega r))}{r} \tag{2}$$

(r is the interacting electrons distance, α and β are functional parameters, and ω is the system-dependent range switching parameter.) For the energy expression, as usually affected in RSH functionals, we use the exact (Fock) exchange for the first term, noted below as $E_{\mathrm{F_X}}$, and a semilocal density exchange functional of choice for the second term, noted below as $E_{\mathrm{DF_X}}$. The SRSH exchange−correlation functional is then written as

$$E_{\mathrm{XC}}^{\mathrm{SRSH}} = \alpha E_{\mathrm{F_X}}^{\mathrm{SR}} + (1-\alpha)E_{\mathrm{DF_X}}^{\mathrm{SR}} + (\alpha+\beta)E_{\mathrm{F_X}}^{\mathrm{LR}} + (1-\alpha-\beta)E_{\mathrm{DF_X}}^{\mathrm{LR}} + E_{\mathrm{DF_C}} \tag{3}$$

In the preceding expression, we add the superscript for the LR and SR of the exact and functional exchange terms and noted the correlation term by $E_{\mathrm{DF_C}}$.

In RSH functionals the OT finds the ω that minimizes the error measure on the basis of the orbital and ionization energies, with a particular choice of the α and β parameters.[34] For example the expression can be defined as follows:

$$J_{\mathrm{OT}}{}^2(\omega) = [E_{\mathrm{HOMO}}(\omega) + \mathrm{IP}(\omega)]^2 + [E_{\mathrm{LUMO}}(\omega) + \mathrm{EA}(\omega)]^2 \tag{4}$$

where E_{HOMO} and E_{LUMO} denote the energies of the HOMO and LUMO, and IP and EA are the vertical ionization potential and electron affinity of the system, respectively.

The SRSH-PCM framework as detailed in ref 38, where the condensed phase represented by a scalar dielectric constant is addressed, uses the range separation parameter obtained by OT for the single molecule in the gas phase with a preset α value. Crucially, in SRSH the functional parameters are then set to address the screened electrostatic interactions using the dielectric constant (ϵ) such that

$$\alpha + \beta = 1/\epsilon \tag{5}$$

thereby establishing the LR weight of the exact exchange in eq 3. In this way the electronic density polarization due to the dielectric environment is addressed by the same constant in the PCM and the functional expression. More specifically, within SRSH the β is reset to correspond to the ϵ using a preset value of α ($\beta = 1/\epsilon - \alpha$). Below we use α values within the 0.2−0.4 range.

Excited-state energies are calculated at the perturbative linear response (ptLR) level where only the first order response to the reaction field representing the dielectric

https://dx.doi.org/10.1021/acs.jctc.0c00086
J. Chem. Theory Comput. XXXX, XXX, XXX−XXX

environment is invoked.[50] In all of the TDDFT calculations we set the optical dielectric constant to 1.88, unless noted otherwise. All of the calculations were performed using Q-Chem[51] and the cc-pVDZ basis set. Molecular geometries are optimized at the B3LYP/cc-PVDZ level of theory with the coordinates included in the Supporting Information (SI).

The set of benchmark molecules is illustrated in Figure 1. Primarily, we address the molecules in the solvent that was

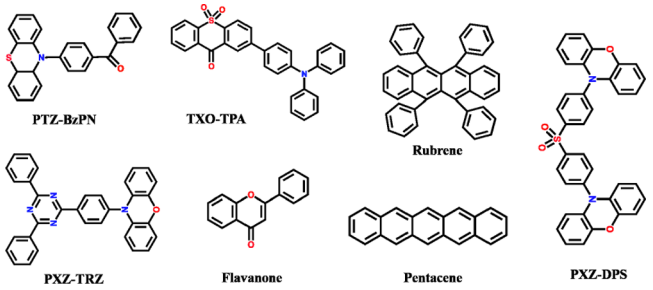

Figure 1. Benchmark set of molecules. Atomic Cartesian coordinates of the optimized geometries at the B3LYP/cc-PVDZ level are provided in the SI.

used in the referenced experimental studies as noted next. More specifically the measured triplet energies are of the following molecules: TXO-TPA (9-*H*-thioxanthen-9-one-10,10-dioxide triphenylamine),[52,53] PXZ-TRZ (10-(4-(4,6-diphenyl-1,3,5-triazin-2-yl)phenyl)-10*H*-phenoxazine),[53,54] PTZ-BzPN (4-(10*H*-phenothiazin-10-yl)phenyl)(phenyl)-methanone),[48] PXZ-DPS (diphenoxazine diphenylsulfone),[55] flavanone,[56] rubrene,[57,58] and pentacene.[59,60] We also address the molecules in their crystal phase by considering their own dielectric constant as evaluated using Clausius−Mossotti equation,[61−63] which relates the dielectric constant to the molecular dipole and polarizability.[61] See the solvents and dielectric constants addressed for each of the benchmark molecules and the molecular crystal-phase dielectric constants listed in SI Table S1.

RESULTS AND DISCUSSION

We begin by addressing these molecules in gas-phase calculations. The corresponding J_{OT} and J_{TT} error measures for these molecules are illustrated in Figure 2 with the numerical values listed in SI Table S2. As expected, we confirm the success of the RSH approach to present low-J_{OT} errors with the average for the considered set well below 0.05 eV, whereas the mean is close to 0.1 eV for HF and B3LYP. The orbital gap energies with HF and B3LYP are overestimated and underestimated, respectively, leading to similar average absolute deviation. (The complete list of the energies used to calculate the J_{OT} measures is provided in SI Table S3).

These trends are even more pronounced for J_{TT}, the triplet gap error measure. The J_{TT} errors are on average larger than 0.3 eV for both HF and B3LYP. The T1 excitation energies are overestimated by HF, while these appear to be underestimated by the B3LYP values. Importantly with RSH the error measures are smaller at around 0.1 eV and where the tuning is *not* involving any triplet energies.

Interestingly the J_{TT} values appear to be significantly dependent on the α parameter, while the RSH error measures based on α in the 0.2−0.4 range remain smaller than the B3LYP and HF values in spite of the strong α dependence.

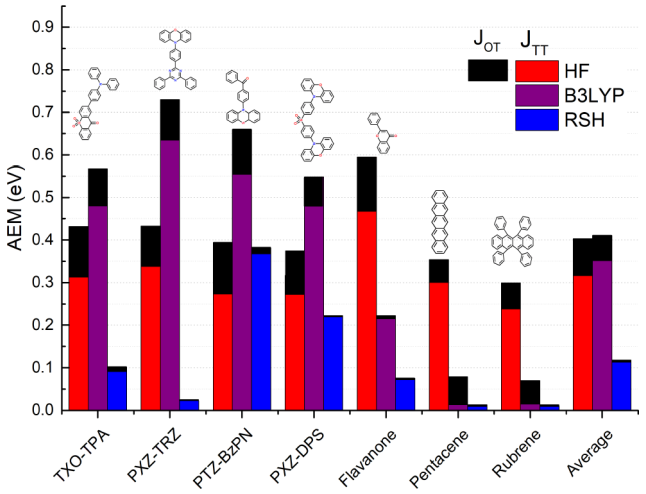

Figure 2. Gas-phase error measures (represented by bars), J_{OT} and J_{TT}, at HF, B3LYP, and RSH levels. J_{OT} is provided at the top part of each bar in black. The numerical values are listed in SI Table S2. The corresponding energies of HOMO/IP, LUMO/EA, and ΔE_{st}(SCF) and E_{T1} are provided in SI Tables S3 and S4 (eV).

Figure 2 presents energies calculated with $\alpha = 0.3$. (The J_{OT} are the smallest at $\alpha = 0.3$.) Not surprising the RSH J_{OT} measure shows weaker dependence on α since this measure is directly addressed in the tuning. Nevertheless, we point out the stronger α dependence of the triplet measure as an indicator for the prospect to further enhance the performance by affecting the tuning with triplet energies.

We next proceed to consider the different levels where PCM is invoked to address the solvated molecules. Namely, PCM is invoked with the scalar dielectric constant, ϵ, corresponding to the relevant solvent for each molecule as listed above in SI Table S1. The PCM J_{OT} and J_{TT} error measures are illustrated in Figure 3 with the values listed in SI Table S5 and the corresponding energies listed in SI Tables S6 and S7. Most pronounced are the larger error measures for the HF triplet

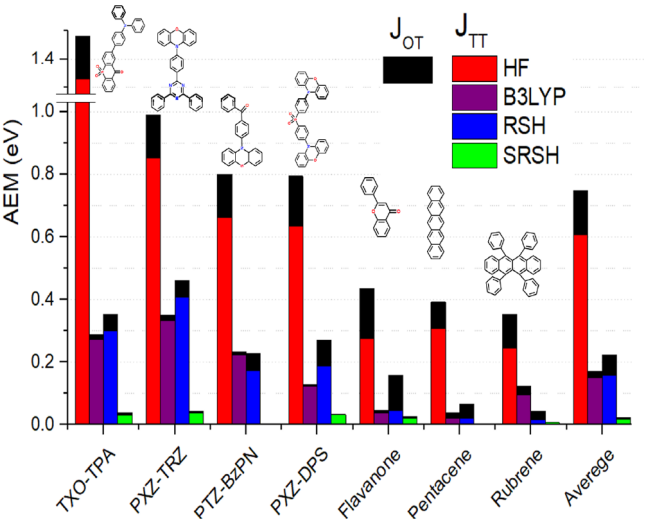

Figure 3. PCM-based error measures (represented by bars), J_{OT} and J_{TT}, at HF, B3LYP, RSH, and SRSH with PCM levels. J_{OT} is provided at the top of each bar in black. The numerical values are listed in SI Table S5. The corresponding energies of HOMO/IP, LUMO/EA, and ΔE_{st}(SCF) and E_{T1} are provided in SI Tables S6 and S7 (eV).

https://dx.doi.org/10.1021/acs.jctc.0c00086
J. Chem. Theory Comput. XXXX, XXX, XXX−XXX

energies. Here we find an average deviation close to 0.8 eV due to the overestimation of the excited triplet-states energies. The average deviation is quite significant for RSH-PCM and B3LYP (in PCM) at 0.2 eV. The SRSH-PCM, on the other hand, presents a significant improvement with the mean error, dropping to below 0.05 eV.

The triplet excitation energies appear to be significantly affected by the α value similarly to the gas-phase trend discussed above. In Figure 4 we present the SRSH-PCM error

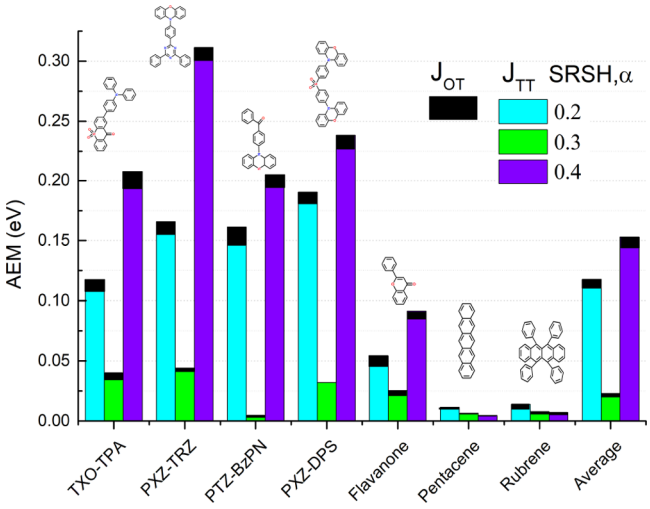

Figure 4. SRSH-PCM-based error measures (represented by bars), J_{OT} and J_{TT}, with various α values. J_{OT} is provided at the top part of each bar in black. The numerical values are listed in SI Table S5. The corresponding energies of HOMO/IP, LUMO/EA, and ΔE_{st}(SCF) and E_{T1} are provided in SI Tables S6 and S7 (eV).

measures with several α values, where 0.3 appears to reduce the measures the most. Note that similarly to the gas-phase trend the SRSH-PCM J_{TT} error measures with all of the considered α parameters remain smaller than the B3LYP and HF errors (again in spite of the relatively significant effect due to the α value). We also find that the optimal α based on J_{TT} appears to correspond to that based on the J_{OT} measure, where rubrene appears to show a slight deviation from this trend. The corresponding energies are included in SI Tables S5−S7. Nevertheless, the relatively significant dependence of PCM-based J_{TT} on the α confirms that the functional parameter space does offer a means to enhance the performance by optimally tuning within PCM. An aspect that is not explored in this study, where tuning is based on the fundamental gap and ionization energies.

We proceed to consider the dependence of the triplet-state energies and error measures of the different PCM levels as ϵ is varied. Specifically J_{TT} measures for all considered molecules at the dielectric constants of the relevant solutions and of their own crystal phases as listed in SI Table S1 are provided. For illustration we follow the error measure trends for TXO-TPA of 4.68 coulomb·m dipole moment calculated in the solid-phase dielectric, where the triplet excited state is associated with CT between donor and acceptor sites of 0.907e and 0.765e in the solid phase and in the solution, respectively. In general states associated with significant CT are expected to strongly depend on the dielectric constant. As shown in Figure 5 only with SRSH-PCM the T1 state energies depend on the dielectric constant, whereas for B3LYP and RSH (with PCM),

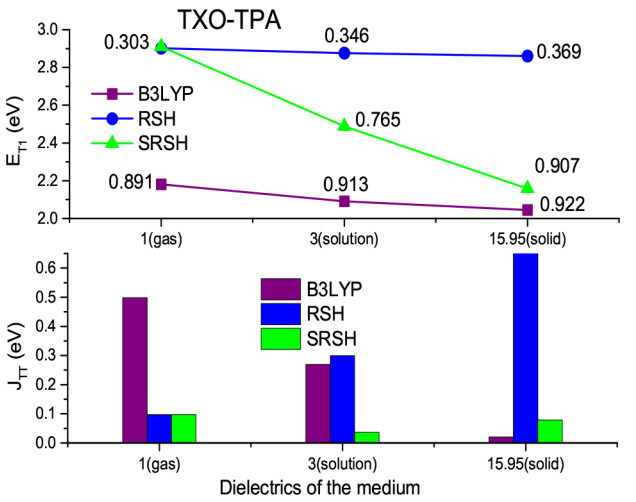

Figure 5. TXO-TPA. Lower: Error measures at gas, solvated, and solid phases (see dielectric constants listed in SI Table S1) at RSH, B3LYP, and SRSH PCM levels. J_{TT} values are listed in SI Tables S4, S7, and S8, respectively. Upper: Triplet excitation energies (E_{T1}) (eV) with their charge transfer noted. The values are listed in SI Table S9, including those of the other molecules.

these energies remain almost the same at the different dielectric constants. The dependence of the triplet excitation energies that is captured by the SRSH-PCM approach leads to error measures that are well below 0.1 eV with all considered constants, whereas the error measures for RSH-PCM and B3LYP vary quite significantly with the constant. For TXO-TPA the B3LYP error measure decreases with the increase of the dielectric constant starting with an error of 0.5 eV at the gas phase, whereas with RSH-PCM the error appears to increase with the constant to 0.6 eV at the larger considered dielectric constant of 15.95. Similar trends are noted for the other molecules and are provided within SI Figure S1.

Importantly, the significantly smaller J_{TT} indicated for SRSH-PCM improves the agreement of the calculated triplet excitations with measured excitation energies. The deviation of the calculated triplet excitation energies from the reported excitations in solution are represented in Figure 6, where the excitation energies are also indicated. See the energies listed in SI Table S9 including values at gas-, solution-, and solid-phase dielectric constants. The SRSH-PCM energies are found to be within 0.1 eV from the measured values (with the exception of PXZ-DPS), whereas RSH energies overestimate by 0.3 eV (for three of the molecules) and B3LYP energies appear to underestimate the energies. As demonstrated in the SI table the molecules associated with larger dipole moment and polarizability and consequently the excited state of significant charge transfer (TXO-TPA, PXZ-TRZ, PTZ-BzPN,and PXZ-DPS) are strongly dependent on the dielectric constant (again a feature correctly established only by the SRSH-PCM), whereas the molecules of vanishing dipole moment and charge transfer present a weak to vanishing dependence on the dielectric constant.

As a final point we emphasize that the SRSH-PCM framework stands on the consistent treatment of the polarization due to the dielectric environment that is represented by a scalar dielectric constant. The same constant is invoked both in the self-consistent reaction field and in screening the LR exact exchange in the functional. Indeed the excellent performance reported above for the triplet excitation

https://dx.doi.org/10.1021/acs.jctc.0c00086
J. Chem. Theory Comput. XXXX, XXX, XXX−XXX

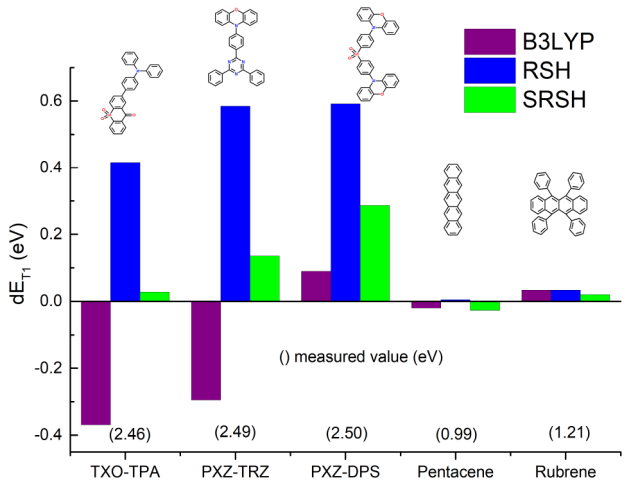

Figure 6. Deviation of solution-phase-calculated triplet excitation energies from spectral measured values at the B3LYP, RSH, and SRSH ($\alpha = 0.3$) levels. The measured excitation energies are indicated in parentheses (eV). The numerical values are included in SI Table S9.

energies is *not* based on affecting the parameter tuning by triplet energies. In fact, we confirm that the J_{TT} measure is minimal at the optimal set of functional parameters determined by J_{OT}, where only rubrene appears to present an insignificant deviation of this trend (see SI Table S5). As a result the success in calculating the triplet energies is achieved in addition to the high-quality performance in addressing singlet excitations including those with a CT character.[39,70−72]

To illustrate this important point, we address here also singlet-state excitation energies for the pentacene system that appears to be a challenging case drawing a wide research effort.[59,64,66,67] Table 1 presents both singlet and triplet excitation energies at the B3LYP, RSH-PCM, and SRSH-PCM levels with a scalar dielectric constant of 2.0 corresponding to hexane as the solvent. As seen in the table the measured low-lying singlet excitation energy of 2.3 eV[65] is reproduced well by SRSH-PCM, whereas a lower measured 1.8 eV[64] excitation appears to have resulted from an aggregation effect[59] that is not addressed by our calculations. Interestingly, the lower lying excitation of 1.8 eV appears to be due to an excitonic state affected by aggregation. Indeed, this value is in agreement with crystal-phase measurements and addressing its excitonic nature is beyond the scope of this work. Interestingly, the triplet excitation appears to show a weak dependence on the dielectric constant, where the gas-phase excitation is essentially the same as the PCM values. For the singlet case the gas-phase excitation is 2.53 eV, which is almost 0.2 eV larger than that for the hexane-solvated value.

CONCLUSIONS

In this study, we demonstrate for the first time the success of the SRSH-PCM framework in the calculation of triplet excited states in the condensed phase. The success of the approach stems from the polarization consistent scheme that was recently reported for the calculation of condensed-phase orbital gaps and CT states. The error measure, J_{TT}, reflecting the deviation of TDDFT-calculated triplet excited-states energies (E_{T1}) from the singlet−triplet energy gap, is found to be smaller than 0.1 eV for all considered molecules and dielectric constants on the basis of SRSH-PCM, while alternative PCM levels are associated with significantly larger deviations. Importantly, the success of SRSH-PCM is demonstrated with OT that is based only on the orbital and ionization energies calculated at the gas phase. Therefore, the excellent performance demonstrated for the excited-state triplet energies is achieved in addition to the already demonstrated success in calculating singlet excited states.[39,70] The prospect for further tightening of the triplet energy accuracy where the tuning is also affected by triplet energies is demonstrated by considering the trends with several values of the α parameter. Specifically, $\alpha = 0.3$ is found to be optimal for all of the molecules at the various condensed phases considered in this benchmark.

ASSOCIATED CONTENT

Supporting Information

The Supporting Information is available free of charge at https://pubs.acs.org/doi/10.1021/acs.jctc.0c00086.

Numerical values of the error measures and the excitation energies used to evaluate the error measures; benchmark measured values and listing of the dielectric constants corresponding to the considered solution and solid phase; atomic coordinates of the different molecules (PDF)

AUTHOR INFORMATION

Corresponding Author

Barry D. Dunietz − *Department of Chemistry and Biochemistry, Kent State University, Kent, Ohio 44242, United States;* orcid.org/0000-0002-6982-8995; Phone: +1 330 6722032; Email: bdunietz@kent.edu; Fax: +1 330 6723816

Authors

Khadiza Begam − *Department of Physics, Kent State University, Kent, Ohio 44242, United States*

Srijana Bhandari − *Department of Chemistry and Biochemistry, Kent State University, Kent, Ohio 44242, United States*

Buddhadev Maiti − *Department of Chemistry and Biochemistry, Kent State University, Kent, Ohio 44242, United States*

Complete contact information is available at:

Table 1. Pentacene Solvent-Phase Singlet and Triplet Energies

		RSH gas at α	RSH-PCM gas at α		SRSH-PCM at α			
state	B3LYP-PCM	0.3	0.2	0.3	0.2	0.3	0.4	Exp.
T1	0.973	0.994	1.023	0.995	0.982	0.964	0.946	0.99[a]
S1	2.083	2.526	2.443	2.428	2.235	2.269	2.320	1.80[a], 2.31[b], 2.37[c]

[a]Measured values in hexane.[60,64] The reported low-lying singlet excitation energy of 1.80 eV appears to be affected by aggregation as it is close to the excitation energy of 1.83 eV reported for the polycrystalline phase of pentacene.[59] [b]Single molecule measurement using molecular beam.[65,66] [c]Extrapolated gas-phase measured value based on solvation correction.[67−69]

https://dx.doi.org/10.1021/acs.jctc.0c00086
J. Chem. Theory Comput. XXXX, XXX, XXX−XXX

https://pubs.acs.org/10.1021/acs.jctc.0c00086

Notes

The authors declare no competing financial interest.

■ ACKNOWLEDGMENTS

B.D.D. acknowledges support for this project by the Department of Energy (DOE)—Basic Energy Sciences through the Chemical Sciences Geosciences and Biosciences Division, through Grant No. DE-SC0016501. We are also grateful to generous resource allocations on the Ohio Supercomputer Center[73] and the Kent State University, College of Arts and Sciences Computing Cluster. K.B. is grateful to Huseyin Aksu for his help and support.

■ REFERENCES

(1) Janata, J.; Josowicz, M. Organic semiconductors in potentiometric gas sensors. *J. Solid State Electrochem.* **2009**, *13*, 41.
(2) Lunt, R. R.; Benziger, J. B.; Forrest, S. R. Relationship between crystalline order and exciton diffusion length in molecular organic semiconductors. *Adv. Mater.* **2010**, *22*, 1233−1236.
(3) Lu, N.; Li, L.; Liu, M. A review of carrier thermoelectric-transport theory in organic semiconductors. *Phys. Chem. Chem. Phys.* **2016**, *18*, 19503−19525.
(4) Uoyama, H.; Goushi, K.; Shizu, K.; Nomura, H.; Adachi, C. Highly efficient organic light-emitting diodes from delayed fluorescence. *Nature* **2012**, *492*, 234.
(5) Bousquet, D.; Fukuda, R.; Jacquemin, D.; Ciofini, I.; Adamo, C.; Ehara, M. Benchmark study on the triplet excited-state geometries and phosphorescence energies of heterocyclic compounds: comparison between TD-PBE0 and SAC-CI. *J. Chem. Theory Comput.* **2014**, *10*, 3969−3979.
(6) Endo, A.; Sato, K.; Yoshimura, K.; Kai, T.; Kawada, A.; Miyazaki, H.; Adachi, C. Efficient up-conversion of triplet excitons into a singlet state and its application for organic light emitting diodes. *Appl. Phys. Lett.* **2011**, *98*, 083302.
(7) Peach, M. J.; Williamson, M. J.; Tozer, D. J. Influence of triplet instabilities in TDDFT. *J. Chem. Theory Comput.* **2011**, *7*, 3578−3585.
(8) Cui, L.-S.; Ruan, S.-B.; Bencheikh, F.; Nagata, R.; Zhang, L.; Inada, K.; Nakanotani, H.; Liao, L.-S.; Adachi, C. Long-lived efficient delayed fluorescence organic light-emitting diodes using n-type hosts. *Nat. Commun.* **2017**, *8*, 2250.
(9) Wex, B.; Kaafarani, B. R. Perspective on carbazole-based organic compounds as emitters and hosts in TADF applications. *J. Mater. Chem. C* **2017**, *5*, 8622−8653.
(10) Thirion, D.; Kasparek, C.; Baumann, T. *45.3: TADF Emitters for Deep-Blue OLEDs. SID Symposium Digest of Technical Papers*; John Wiley and Sons: Hoboken, NJ, USA, 2019; Vol. *50*, pp 497−499, DOI: 10.1002/sdtp.13542.
(11) Runge, E.; Gross, E. K. U. Density-functional theory for time-dependent systems. *Phys. Rev. Lett.* **1984**, *52*, 997−1000.
(12) Geerlings, P.; De Proft, F.; Langenaeker, W. Conceptual density functional theory. *Chem. Rev.* **2003**, *103*, 1793−1874.
(13) Burke, K.; Werschnik, J.; Gross, E. K. U. Time-dependent density functional theory: Past, present, and future. *J. Chem. Phys.* **2005**, *123*, 062206.
(14) Casida, M. E. Time-dependent density-functional theory for molecules and molecular solids. *J. Mol. Struct.: THEOCHEM* **2009**, *914*, 3−18.
(15) Egger, D. A.; Weissman, S.; Refaely-Abramson, S.; Sharifzadeh, S.; Dauth, M.; Baer, R.; Kümmel, S.; Neaton, J. B.; Zojer, E.; Kronik, L. Outer-Valence Electron Spectra of Prototypical Aromatic Heterocycles From an Optimally-Tuned Range-Separated Hybrid Functional. *J. Chem. Theory Comput.* **2014**, *10*, 1934.
(16) Perdew, J. P.; Levy, M. Physical Content of the Exact Kohn-Sham Orbital Energies: Band Gaps and Derivative Discontinuities. *Phys. Rev. Lett.* **1983**, *51*, 1884−1887.
(17) Sham, L. J.; Schlüter, M. Density Functional Theory of the Gap. *Phys. Rev. Lett.* **1983**, *51*, 1888−1891.
(18) Seidl, A.; Görling, A.; Vogl, P.; Majewski, J. A.; Levy, M. Generalized Kohn-Sham Schemes and the Band-Gap Problem. *Phys. Rev. B: Condens. Matter Mater. Phys.* **1996**, *53*, 3764−3774.
(19) Kümmel, S.; Kronik, L. Orbital-Dependent Density Functionals: Theory and Applications. *Rev. Mod. Phys.* **2008**, *80*, 3−60.
(20) Jacquemin, D.; Perpete, E. A.; Ciofini, I.; Adamo, C. Assessment of functionals for TD-DFT calculations of singlet- triplet transitions. *J. Chem. Theory Comput.* **2010**, *6*, 1532−1537.
(21) Niehaus, T. A.; Hofbeck, T.; Yersin, H. Charge-transfer excited states in phosphorescent organo-transition metal compounds: a difficult case for time dependent density functional theory? *RSC Adv.* **2015**, *5*, 63318−63329.
(22) Jacquemin, D.; Adamo, C. *Density-Functional Methods for Excited States*; Springer: Cham, Switzerland, 2015; pp 347−375, DOI: 10.1007/128_2015_638.
(23) Dreuw, A.; Weisman, J.; Head-Gordon, M. Long-range charge-transfer excited states in time-dependent density functional theory require non-local exchange. *J. Chem. Phys.* **2003**, *119*, 2943−2946.
(24) Chai, J.-D.; Head-Gordon, M. Systematic Optimization of Long-Range Corrected Hybrid Density Functionals. *J. Chem. Phys.* **2008**, *128*, 084106.
(25) Chai, J.-D.; Head-Gordon, M. Long-Range Corrected Hybrid Density Functionals With Damped Atom-Atom Dispersion Corrections. *Phys. Chem. Chem. Phys.* **2008**, *10*, 6615.
(26) Stein, T.; Kronik, L.; Baer, R. Prediction of Charge-Transfer Excitations in Coumarin-Based Dyes Using a Range-Separated Functional Tuned From First Principles. *J. Chem. Phys.* **2009**, *131*, 244119.
(27) Kronik, L.; Stein, T.; Refaely-Abramson, S.; Baer, R. Excitation Gaps of Finite-Sized Systems from Optimally Tuned Range-Separated Hybrid Functionals. *J. Chem. Theory Comput.* **2012**, *8*, 1515−1531.
(28) Refaely-Abramson, S.; Baer, R.; Kronik, L. Fundamental and excitation gaps in molecules of relevance for organic photovoltaics from an optimally tuned range-separated hybrid functional. *Phys. Rev. B: Condens. Matter Mater. Phys.* **2011**, *84*, 075144.
(29) Kuritz, N.; Stein, T.; Baer, R.; Kronik, L. Charge-Transfer-Like $\pi - \pi^*$ Excitations in Time-Dependent Density Functional Theory: A Conundrum and Its Solution. *J. Chem. Theory Comput.* **2011**, *7*, 2408−2415.
(30) Koopmans, T. Über die Zuordnung von Wellenfunktionen und Eigenwerten zu den einzelnen Elektronen eines Atoms. *Physica* **1934**, *1*, 104−113.
(31) Heinrich, N.; Koch, W.; Frenking, G. On the use of Koopmans' theorem to estimate negative electron affinities. *Chem. Phys. Lett.* **1986**, *124*, 20−25.
(32) Manna, A. K.; Refaely-Abramson, S.; Reilly, A. M.; Tkatchenko, A.; Neaton, J. B.; Kronik, L. Quantitative Prediction of Optical Absorption in Molecular Solids from an Optimally Tuned Screened Range-Separated Hybrid Functional. *J. Chem. Theory Comput.* **2018**, *14*, 2919−2929.
(33) Refaely-Abramson, S.; Jain, M.; Sharifzadeh, S.; Neaton, J. B.; Kronik, L. Solid-State Optical Absorption From Optimally Tuned Time-Dependent Range-Separated Hybrid Density Functional Theory. *Phys. Rev. B: Condens. Matter Mater. Phys.* **2015**, *92*, 081204−081209.
(34) Refaely-Abramson, S.; Sharifzadeh, S.; Jain, M.; Baer, R.; Neaton, J. B.; Kronik, L. Gap Renormalization of Molecular Crystals From Density-Functional Theory. *Phys. Rev. B: Condens. Matter Mater. Phys.* **2013**, *88*, 081204.
(35) Lüftner, D.; Refaely-Abramson, S.; Pachler, M.; Resel, R.; Ramsey, M. G.; Kronik, L.; Puschnig, P. *Phys. Rev. B: Condens. Matter Mater. Phys.* **2014**, *90*, 075204−075213.
(36) Kronik, L.; Neaton, J. B. Excited-State Properties of Molecular Solids from First Principles. *Annu. Rev. Phys. Chem.* **2016**, *67*, 587−616.
(37) Zheng, Z.; Egger, D. A.; Brédas, J.-L.; Kronik, L.; Coropceanu, V. Effect of Solid-State Polarization on Charge-Transfer Excitations

and Transport Levels at Organic Interfaces From a Screened Range-Separated Hybrid Functional. *J. Phys. Chem. Lett.* **2017**, *8*, 3277−3283.
(38) Bhandari, S.; Cheung, M.; Geva, E.; Kronik, L.; Dunietz, B. D. Fundamental Gaps of Condensed-Phase Organic Semiconductors From Single-Molecule Polarization-Consistent Optimally Tuned Screened Range-Separated Hybrid Functionals. *J. Chem. Theory Comput.* **2018**, *14*, 6287−6294.
(39) Bhandari, S.; Dunietz, B. D. Quantitative Accuracy in Calculating Charge Transfer State Energies in Solvated Molecular Dimers Using Screened Range Separated Hybrid Functional Within a Polarized Continuum Model. *J. Chem. Theory Comput.* **2019**, *15*, 4305.
(40) Joo, B.; Han, H.; Kim, E.-G. Solvation-Mediated Tuning of the Range-Separated Hybrid Functional: Self-Sufficiency through Screened Exchange. *J. Chem. Theory Comput.* **2018**, *14*, 2823−2828.
(41) Gourdon, G.; Radvanyi, F.; Lia, A.-S.; Duros, C.; Blanche, M.; Abitbol, M.; Junien, C.; Hofmann-Radvanyi, H. Moderate intergenerational and somatic instability of a 55-CTG repeat in transgenic mice. *Nat. Genet.* **1997**, *15*, 190−192.
(42) Szalay, P. G.; Vazquez, J.; Simmons, C.; Stanton, J. F. Triplet instability in doublet systems. *J. Chem. Phys.* **2004**, *121*, 7624−7631.
(43) Peach, M. J.; Tozer, D. J. Overcoming low orbital overlap and triplet instability problems in TDDFT. *J. Phys. Chem. A* **2012**, *116*, 9783−9789.
(44) Budworth, H.; McMurray, C. T. A Brief History of Triplet Repeat Diseases. *Trinucleotide Repeat Protocols*; Springer: New York, 2013; pp 3−17, DOI: 10.1007/978-1-62703-411-1_1.
(45) Yamada, T.; Hirata, S. Singlet and triplet instability theorems. *J. Chem. Phys.* **2015**, *143*, 114112.
(46) Sears, J. S.; Koerzdoerfer, T.; Zhang, C.-R.; Brédas, J.-L. Communication: Orbital instabilities and triplet states from time-dependent density functional theory and long-range corrected functionals. *J. Chem. Phys.* **2011**, *135*, 151103.
(47) Korzdorfer, T.; Bredas, J.-L. Organic electronic materials: recent advances in the DFT description of the ground and excited states using tuned range-separated hybrid functionals. *Acc. Chem. Res.* **2014**, *47*, 3284−3291.
(48) Han, H.; Kim, E.-G. Dielectric Effects on Charge-Transfer and Local Excited States in Organic Persistent Room-Temperature Phosphorescence. *Chem. Mater.* **2019**, *31*, 6925−6935.
(49) Lin, Z.; Van Voorhis, T. Triplet Tuning: ANovel Family of Non-Empirical Exchange−Correlation Functionals. *J. Chem. Theory Comput.* **2019**, *15*, 1226−1241.
(50) Mewes, J.-M.; You, Z.-Q.; Wormit, M.; Kriesche, T.; Herbert, J. M.; Dreuw, A. Experimental benchmark data and systematic evaluation of two a posteriori, polarizable-continuum corrections for vertical excitation energies in solution. *J. Phys. Chem. A* **2015**, *119*, 5446−5464.
(51) Shao, Y.; Gan, Z.; Epifanovsky, E.; Gilbert, A. T.; Wormit, M.; Kussmann, J.; Lange, A. W.; Behn, A.; Deng, J.; Feng, X.; et al. Advances in Molecular Quantum Chemistry Contained in the Q-Chem 4 Program Package. *Mol. Phys.* **2015**, *113*, 184−215.
(52) Wang, H.; Xie, L.; Peng, Q.; Meng, L.; Wang, Y.; Yi, Y.; Wang, P. Novel thermally activated delayed fluorescence materials−thioxanthone derivatives and their applications for highly efficient OLEDs. *Adv. Mater.* **2014**, *26*, 5198−5204.
(53) Sun, H.; Hu, Z.; Zhong, C.; Chen, X.; Sun, Z.; Bredas, J.-L. Impact of dielectric constant on the singlet-triplet gap in thermally activated delayed fluorescence materials. *J. Phys. Chem. Lett.* **2017**, *8*, 2393−2398.
(54) Tanaka, H.; Shizu, K.; Nakanotani, H.; Adachi, C. Twisted intramolecular charge transfer state for long-wavelength thermally activated delayed fluorescence. *Chem. Mater.* **2013**, *25*, 3766−3771.
(55) Zhang, Q.; Tsang, D.; Kuwabara, H.; Hatae, Y.; Li, B.; Takahashi, T.; Lee, S. Y.; Yasuda, T.; Adachi, C. Nearly 100% internal quantum efficiency in undoped electroluminescent devices employing pure organic emitters. *Adv. Mater.* **2015**, *27*, 2096−2100.
(56) Mabry, T. J.; Markham, K.; Thomas, M. The Ultraviolet Spectra of Flavones and Flavanols. *The systematic identification of flavonoids*; Springer: Berlin, 1970; pp 41−164, DOI: 10.1007/978-3-642-88458-0_5.
(57) Petrenko, T.; Krylova, O.; Neese, F.; Sokolowski, M. Optical absorption and emission properties of rubrene: insight from a combined experimental and theoretical study. *New J. Phys.* **2009**, *11*, 015001.
(58) Pandey, A. K. Highly efficient spin-conversion effect leading to energy up-converted electroluminescence in singlet fission photovoltaics. *Sci. Rep.* **2015**, *5*, 7787.
(59) Rao, A.; Wilson, M. W.; Albert-Seifried, S.; Di Pietro, R.; Friend, R. H. Photophysics of pentacene thin films: The role of exciton fission and heating effects. *Phys. Rev. B: Condens. Matter Mater. Phys.* **2011**, *84*, 195411.
(60) Porter, G.; Windsor, M. W. The triplet state in fluid media. *Proc. R. Soc. A* **1958**, *245*, 238−258.
(61) Onsager, L. Electric moments of molecules in liquids. *J. Am. Chem. Soc.* **1936**, *58*, 1486−1493.
(62) Wyman, J., Jr; Ingalls, E. The dielectric constant of deuterium oxide. *J. Am. Chem. Soc.* **1938**, *60*, 1182−1184.
(63) Nayak, P. K.; Periasamy, N. Calculation of ionization potential of amorphous organic thin-films using solvation model and DFT. *Org. Electron.* **2009**, *10*, 532−535.
(64) Khatymova, L.; Kinzyabulatov, R.; Khvostenko, O. Singlet and triplet transitions in UV absorption spectra of pentacene. *High Energy Chem.* **2018**, *52*, 38−44.
(65) Heinecke, E.; Hartmann, D.; Müller, R.; Hese, A. Laser spectroscopy of free pentacene molecules (I): The rotational structure of the vibrationless S 1leftarrow S 0 transition. *J. Chem. Phys.* **1998**, *109*, 906−911.
(66) Zeng, T.; Hoffmann, R.; Ananth, N. The low-lying electronic states of pentacene and their roles in singlet fission. *J. Am. Chem. Soc.* **2014**, *136*, 5755−5764.
(67) Wong, B. M.; Hsieh, T. H. Optoelectronic and Excitonic Properties of Oligoacenes: Substantial Improvements from Range-Separated Time-Dependent Density Functional Theory. *J. Chem. Theory Comput.* **2010**, *6*, 3704−3712.
(68) Grimme, S.; Parac, M. Substantial Errors from Time-Dependent Density Functional Theory for the Calculation of Excited States of Large pi Systems. *ChemPhysChem* **2003**, *4*, 292.
(69) Biermann, D.; Schmidt, W. Diels-Alder reactivity of polycyclic aromatic hydrocarbons. 1. Acenes and benzologs. *J. Am. Chem. Soc.* **1980**, *102*, 3163−3173.
(70) Aksu, H.; Schubert, A.; Geva, E.; Dunietz, B. D. Explaining Spectral Asymmetries and Excitonic Characters of the Core Pigment Pairs in the Bacterial Reaction Center Using Screened Range-Separated Hybrid Functionals. *J. Phys. Chem. B* **2019**, *123*, 8970−8975.
(71) Aksu, H.; Schubert, A.; Bhandari, S.; Yamada, A.; Geva, E.; Dunietz, B. D. On the Role of the Special Pair in Photosystems as a Charge Transfer Rectifier. *J. Phys. Chem. B* **2020**, *124*, 1987−1994.
(72) Song, Y.; Schubert, A.; Liu, X.; Bhandari, S.; Forrest, S. R.; Dunietz, B. D.; Geva, E.; Ogilvie, J. P. Efficient Charge Generation via Hole Transfer in Dilute Organic Donor−Fullerene Blends. *J. Phys. Chem. Lett.* **2020**, *11*, 2203−2210.
(73) *Ohio Supercomputer Center*, 1987. Ohio Supercomputer Center: Columbus OH; http://osc.edu/ark:/19495/f5s1ph73.

https://dx.doi.org/10.1021/acs.jctc.0c00086
J. Chem. Theory Comput. XXXX, XXX, XXX−XXX